Bioimaging

DOI: 10.1002/ange.201202212

Ytterbium-Based Bioprobes for Near-Infrared Two-Photon Scanning Laser Microscopy Imaging**

Anthony D'Aléo, Adrien Bourdolle, Sophie Brustlein, Teddy Fauquier, Alexei Grichine, Alain Duperray, Patrice L. Baldeck, Chantal Andraud, Sophie Brasselet,* and Olivier Maury**

Dedicated to Dr. Hubert Le Bozec on the occasion of his 60th birthday

For decades, optical microscopy has been an essential tool for biological imaging, and more recently luminescence-based techniques have gained widespread use for medical analyses and diagnostics.[1] Conventional one-photon microscopy using commercial bioprobes or fluorescent proteins generally proceeds using excitation wavelength in the UV or visible and detection in the visible spectral range. These microscopy configurations will be referred to as UV-to-visible or visible-to-visible according to the excitation-to-detection spectral ranges. Since biological tissues strongly absorb and scatter UV/visible light, such configurations are restricted to surface bioimaging experiments, for example, 2D cell imaging. On the other hand, the transparency of biological tissues in the near-infrared (NIR) between 700 and 1200 nm, a region called biological window, allows in-depth imaging in this spectral range.[2] Therefore, numerous academic and industrial research endeavors are currently focused on the improvement of microscopy techniques and on the design of new luminescent bioprobes featuring both excitation and emission in this NIR spectral range. Microscopy in this NIR-to-NIR configuration will enable in depth imaging in thick tissues and several bioprobes (cyanine, (aza)-bodipy) combining NIR excitation and emission have been developed and commercialized this last decade.[3] However in these cases, the small Stokes shift between the excitation and the optimal collection range of emitted light is a real technical drawback for microscopy because of the need to cleanly separate the emission from the excitation. Nonlinear biphotonic excitation, that is the simultaneous absorption of two photons of half energy typically in the NIR region, inherently introduces a larger Stokes shift and is therefore an elegant way to circumvent this drawback.[4] However, up to now, all the designed chromophores exhibit an emission in the visible spectral range, and the currently available biphotonic microscopes work in this two-photon NIR-to-visible configuration with a detection wavelength shorter than the incident laser wavelength.[4,5]

In this context, lanthanide complexes and particularly NIR emitters like ytterbium and neodymium are known to exhibit very large pseudo-Stokes shift,[6a,b] and are therefore potentially well-suited for such two photon NIR-to-NIR imaging purpose. In spite of their generally low luminescence quantum yield, such complexes have already been used for NIR bioimaging applications but with a classical one-photon excitation generally localized in the UV/visible up to 550–600 nm.[6,7] The sensitization of lanthanide luminescence by two-photon absorption (TPA) is currently a challenging field of research but so far, most endeavors were focused on terbium and europium emitting in the green and red spectral region, respectively.[6a,8] With regard to NIR emitters, the proof of concept of ytterbium two-photon sensitization has been first described in the early 2000s by Lakowicz and co-workers.[9] Recently, Wong and co-workers have reported an ytterbium complex that exhibit exceptional luminescence properties in water with a remarkable two-photon cross-section.[10] Interestingly, this complex was successfully used as bioprobe to image HeLa cells by a two-photon microscopy technique, working in the classical NIR-to-visible configuration with the detection centered in the residual emission of the ligand.

Here, we report on the proof-of-concept of two-photon NIR-to-NIR microscopy. To that end, we designed water-soluble ytterbium complexes, containing extended π-conjugated skeleton suitable for two-photon excitation and meanwhile, we built up an unconventional two-photon NIR-to-NIR microscopy set-up.

[*] Dr. A. D'Aléo, Dr. A. Bourdolle, Dr. P. L. Baldeck, Dr. C. Andraud, Dr. O. Maury
University Lyon 1, ENS Lyon, CNRS UMR 5182
46 allée d'Italie, 69364 Lyon (France)
E-mail: chantal.andraud@ens-lyon.fr
olivier.maury@ens-lyon.fr

Dr. S. Brustlein, Dr. S. Brasselet
Institut Fresnel, CNRS UMR 6133, Université Aix Marseille III
Ecole Centrale de Marseille. Domaine Universitaire St Jérôme
13397 Marseille cedex 20 (France)
E-mail: sophie.brasselet@fresnel.fr

Dr. A. Grichine, Dr. A. Duperray
Institut Albert Bonniot, INSERM-U823-CHU Grenoble-EFS
Université Joseph Fourier—Grenoble I
BP170, 38042 Grenoble (France)

Dr. T. Fauquier
Institut de Génomique Fonctionnelle de Lyon, Université de Lyon
CNRS, INRA, Ecole Normale Supérieure de Lyon
46 allée d'Italie, 69364 Lyon (France)

[**] We are grateful to Drs Y. Guyot and A. Brenier (LPCML, University of Lyon) for their help with the near-infrared luminescence decay measurements. We also thank F. Albrieux, C. Duchamp, and N. Henriques (University of Lyon) for the assistance and access to the high-resolution mass spectrometry facility.

Supporting information for this article, including synthetic procedures and characterization, spectroscopic and microscopic experimental details, and the preparation of the biological samples, is available on the WWW under http://dx.doi.org/10.1002/anie.201202212.

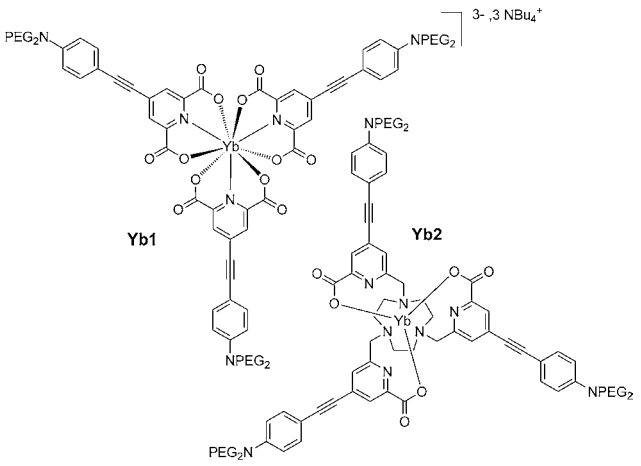

Figure 1. Structure of the target complexes.

The target complexes (Figure 1) need to fulfill some requirements to be used as bioprobe, ideally efficient two-photon antenna, high thermodynamic and kinetic stability, and good photophysical properties. For initial spectroscopy and microscopy experiments, we chose to use the previously described[11] **Yb¹** complex containing bis-PEGamino-(phenyl-ethynyl)-dipicolinic ligands in spite of its limited water stability.[12] In a second time, the analogous macrocylic complex, **Yb²** based on the triaza-cyclononane plateform[13] was designed to increase the stability in biological medium (see the Supporting Information for synthetic details[14] and characterization).

In both cases, the UV/visible absorption spectra show a broad intense transition at 400 nm, assigned to an intraligand charge-transfer (ILCT) transition from the dialkylamino donor part to the chelated dipicolinic electron-withdrawing fragment (Figure 2 and Figure S2 in the Supporting Information). As already observed,[11] the steady-state luminescence spectra obtained by excitation in this ILCT transition is composed of two emission bands: 1) the characteristic ytterbium (III) emission, arising from the $^2F_{5/2} \rightarrow {}^2F_{7/2}$ (980 nm) transition in the NIR spectral range and 2) the broad residual ILCT emission around 600 nm, indicating that the energy transfer to the central metal ion is not complete. The luminescence lifetime associated to the NIR transition was found to be perfectly mono-exponential, with a value of 0.34 and 3 μs for **Yb¹** and **Yb²**, respectively (Figure S3 in the Supporting Information), this later value being in the range of best complexes already reported in water.[10,15] The strong improvement between the two complexes **Yb¹** and **Yb²** featuring similar antenna can be ascribed to the increased stability of the macrocyclic derivative.[13] Under femtosecond Ti:Sa laser irradiation in the 700–900 nm spectral range (Figure S4), an identical luminescence profile is obtained (Figure 2d) with NIR emission observed at a longer wavelength relative to that of the incident laser wavelength (i.e. unusual spectral configuration for TPA-induced luminescence with $\lambda^{det} > \lambda^{ex}$). The quadratic dependence of both residual ILCT and Yb^{III} emission intensities versus the laser power (Figure 2e) unambiguously established that the NIR Yb^{III} emission is sensitized by a two-photon antenna effect. The two-photon cross-sections could not be accurately determined because of the weak luminescence quantum yields of both residual ILCT and Yb^{III} emissions (< 1 %), and to the lack of calibration of the TPA experimental setup in the NIR spectral range. However in a first approximation, these cross-sections should lie in the same range as that of the europium or lutetium analogous estimated to 775 and 500 GM at 740 nm, respectively.[11] Therefore the TPA-induced NIR emission of ytterbium is particularly interesting for in-depth bioimaging experiments because both excitation (750–850 nm) and emission (980 nm) are localized in the biological transparency window (NIR-to-NIR configuration).

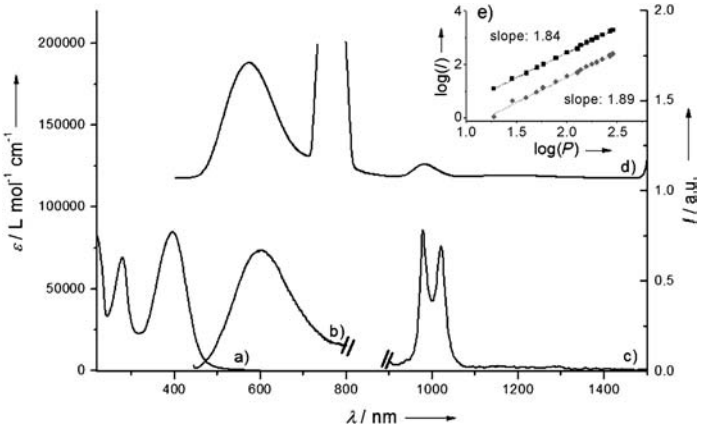

Figure 2. Photophysical data of **Yb¹** in water solution: a) absorption spectrum (scale on the left), b) residual CT fluorescence, and c) NIR emission (λ^{ex} = 380 nm; scale on the right), and d) uncorrected two-photon-induced luminescence spectrum (λ^{ex} = 760 nm; scale on the right). Inset e) shows the variation of the two-photon luminescence intensity with the incident laser power at 573 (■) and 981 nm (●).

Conventional one- and two-photon microscopy imaging experiments were carried out using commercially available epifluorescence and confocal microscopes with either a one-photon excitation in the visible or a two-photon excitation at 760 nm (femtosecond Ti:Sapphire laser). The complex **Yb¹** was incubated with fixed T24 human cancer cells. The one-photon microscopy image (Figure 3a) reveals that the complex successfully stained the cell and localized preferentially in the perinuclear areas or nucleoli as already observed for related europium complexes.[12] The conventional two-photon imaging experiments (Figure 3c) were carried out in the NIR-to-visible configuration using a visible detection at a shorter wavelength than that of the TPA excitation ($\lambda^{det} < \lambda^{ex}$). As expected, this image is very similar to the one-photon one, but the signal-to-noise ratio is higher because the background fluorescence is dramatically reduced using a two-photon excitation. Unfortunately, it was not possible to record any image at the 950–1050 nm emission band because conventional biphotonic microscopes contain optical filtering schemes which do not allow the NIR-to-NIR configuration (that is detection of $\lambda^{det} > \lambda^{ex}$ with both λ^{ex} and λ^{det} in the NIR range). Additionally, the sensitivity of the standard photomultiplier tube (PMT) detectors of the confocal microscope is very low at 980 nm. To tackle these limitations, we developed our own biphotonic microscopy setup based on adequate optical filtering.

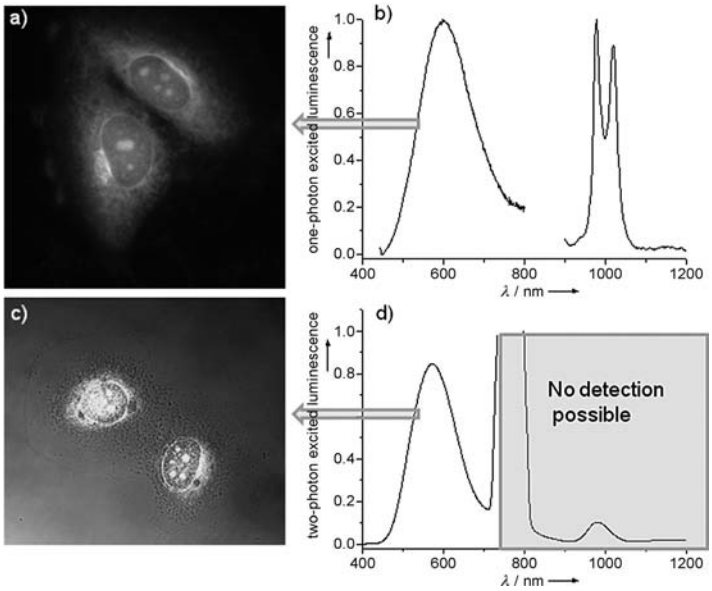

Figure 3. Imaging of the fixed cells stained with **Yb[1]** using a conventional microscope: a) one-photon image using an inverted wide-field microscope ($\lambda^{ex} = 450$–490 nm, visible detection), b,d) one- and two-photon emission spectra (normalized one-photon (b) and two-photon (d) excited luminescence), and c) two-photon NIR-to-visible laser scanning image, ($\lambda^{ex} = 760$ nm, detection in the 491–673 nm range).

The two-photon NIR-to-NIR imaging microscopy setup (Figure 4a) consists in focusing incident pulsed Ti-sapphire laser light (100 fs, 80 MHz, 760 nm wavelength) through a high numerical aperture objective (NA 1.15, water immersion). Images are formed using a galvalnometric scanning over typical regions of 100 μm × 100 μm in the sample plane. To reject as much as possible the incident laser light in the detection channel around 1000 nm, the laser is reflected on a dichroic mirror which transmits the fluorescence emission in the epi descanned detection path. The emission is further filtered by two interference filters, and focused on an avalanche photodiode working in the photon-counting mode. Validation experiments were first carried out using a thin film of **Yb[1]** spread on a glass plate as substrate (Figure 4b). Regions where the film is present are clearly visible with a high signal-to-background ratio relative to the glass substrate. Both the spectrum of emission (Figure 4c) and the incident intensity dependence (Figure 4d) ascertain the detection of NIR light around 1000 nm in the two-photon mode.

As preliminary to the imaging experiments, the influence of this NIR-to-NIR configuration on the depth of penetration in a scattering sample was studied. To that end, the complex **Yb[1]** was dissolved in intralipid solutions of different concentrations, mimicking the scattering ability of the biological media and irradiated by a biphotonic excitation. The variation of the normalized emission intensity in the visible (600 nm) and in the NIR (1000 nm) was measured simultaneously as a function of the depth of the incident laser-focusing position (Figure 5a). As anticipated, the visible emission is more affected by scattering than the NIR emission: at a depth of 100 μm in a strongly scattering medium, almost no visible light is detected whereas more than 20% of the NIR light remains available for imaging purpose. These data are in agreement with recent results comparing the influence of the detection wavelength for a given TPA excitation[16] obtained in a classical TPA configuration ($\lambda^{ex} > \lambda^{det}$). The data shown in Figure 5 are normalized, and usually the NIR detection range exhibits fewer signal than the visible range, because of the lower efficiency of both the imaging setup and the luminescence quantum yield of the complex in this spectral range. Nevertheless, all these experiments unambiguously emphasize the interest of the NIR-to-NIR configuration for in-depth imaging purposes.

To check the potentialities of this two-photon NIR-to-NIR configuration, thick tissue imaging experiments were undertaken. Mouse brain capillary vessels were imaged in depth using the **Yb[2]** as luminescent probes.[17] A phosphate buffer solution of the complex ([C] of about 10^{-4} mol L^{-1}) was directly perfused in the heart of a mouse. Brains were quickly dissected, post-fixed, and slices (100 μm thickness) were cut and conserved between two glass

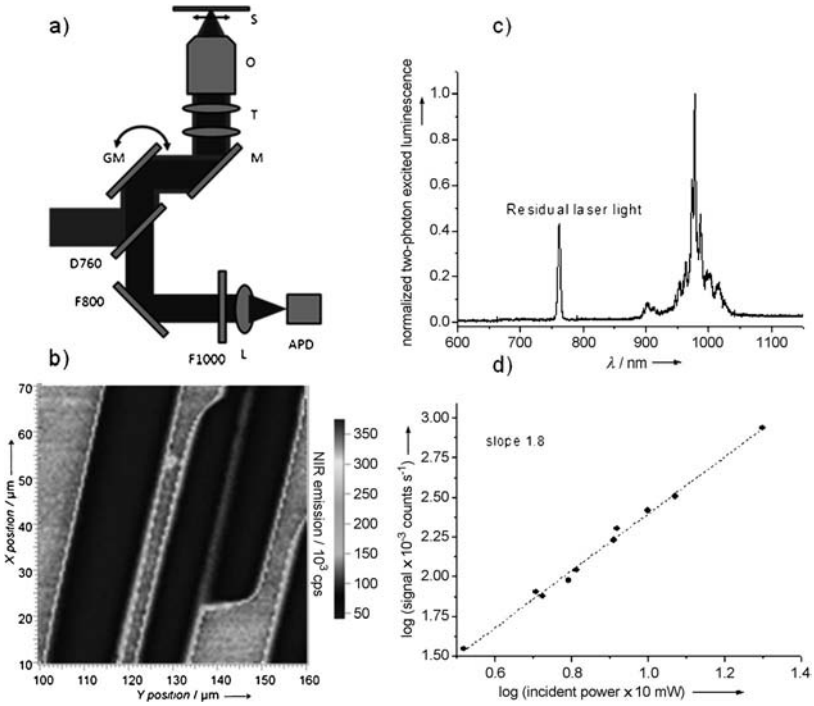

Figure 4. a) Experimental setup for two-photon NIR-to-NIR imaging. O: objective, T: telescope, M: protected silver mirror, GM: galvanometric mirrors, D760: dichroic mirror (FF720-SDi01, Semrock), F800 and F1000: interference filters (800DF50 and 1000DF50, Omega Optical), L: lens, and APD: avalanche photodiode. b) Two-photon scanning image of a thin film of **Yb[1]** on a glass substrate, using a detection wavelength of 1000 nm . c) Spectrum measured in a bright region of the image of (b). A high pass filter at 850 nm is used before the spectrometer. d) Incident power dependence of the fluorescence signal recorded at 1000 nm.

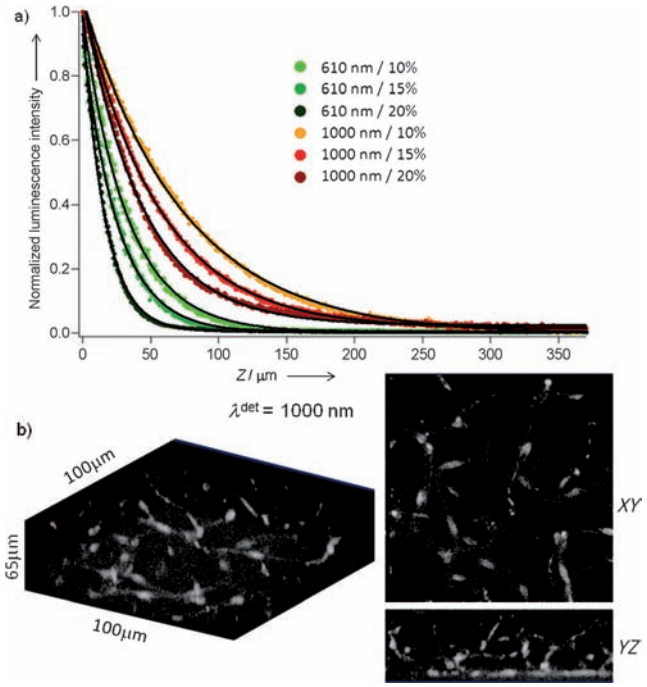

Figure 5. a) Variation of the normalized luminescence intensity of **Yb[1]** at 610 (green) or 1000 nm (red) with the depth of the 760 nm TPA excitation in two intralipid solutions of different concentrations (10%, 15%, 20%) mimicking different scattering strengths. b) 3D biphotonic scanning microscopy image using the home-made setup ($\lambda^{ex} = 760$ nm) of mouse brain slice stained with **Yb[2]** with detection at 1000 nm (incident power 25 mW). Sections of the 3D images of the aforementioned image.

plates. These mouse brain slices were successfully imaged using a biphotonic excitation ($\lambda^{ex} = 760$ nm) and the 3D blood capillary network is observed using the NIR-to-NIR configuration with a detection wavelength at 1000 nm (Figure 5b). This image was recorded at higher laser power to compensate for the lower imaging efficiency in this spectral range. Even though the recorded signal is weak, it shows stained blood vessels with a reasonable signal-to-noise ratio up to 80 µm depths in strongly scattering samples. The integration time of 50 µs per pixel, which is essentially chosen to ensure a high signal-to-noise ratio, could be even more increased to reach a larger imaging depth. This would lead to longer time scales for imaging, however it is possible to reach faster dynamics by using a higher incident power. This result therefore unambiguously establishes the proof-of-concept of two-photon NIR-to-NIR imaging.

In conclusion, we demonstrate the feasibility of in-depth imaging of strongly scattering thick tissue, for example, the vascular network of mouse brain, by two-photon scanning microscopy in an unprecedented NIR-to-NIR configuration. To that end, we developed a new biphotonic setup and we designed a macrocyclic ytterbium complex functionalized by two-photon antenna combining appropriate stability and efficiency in water. Further studies are currently conducted to improve the two-photon brightness of such probes and to expand the scope of this NIR-to-NIR biphotonic microscope.

Received: March 20, 2012
Published online: May 23, 2012

Keywords: bioimaging · biphotonic microscopy · lanthanide complexes · ytterbium

[1] V. Ntziachristos, *Nat. Methods* **2010**, *7*, 603–614.
[2] J. V. Frangioni, *Curr. Opin. Chem. Biol.* **2003**, *7*, 626–634.
[3] a) K. Kiyose, H. Kojima, T. Nagano, *Chem. Asian J.* **2008**, *3*, 506–515; b) S. Achilefu, *Angew. Chem.* **2010**, *122*, 10010–10012; *Angew. Chem. Int. Ed.* **2010**, *49*, 9816–9818; c) H. S. Choi, K. Nasr, S. Alyabyev, D. Feith, J. H. Lee, S. H. Kim, Y. Ashitate, H. Hyun, G. Patonay, L. Strekowski, M. Henary, J. V. Frangioni, *Angew. Chem.* **2011**, *123*, 6382–6387; *Angew. Chem. Int. Ed.* **2011**, *50*, 6258–6263.
[4] a) W. R. Zipfel, R. M. Williams, W. W. Webb, *Nat. Biotechnol.* **2003**, *21*, 1369–1377; b) K. Konig, *J. Microsc.* **2000**, *200*, 83–104.
[5] a) H. M. Kim, B. R. Cho, *Acc. Chem. Res.* **2009**, *42*, 863–872; b) G. S. He, L.-S. Tan, Q. Zheng, P. N. Prasad, *Chem. Rev.* **2008**, *108*, 1245–1330.
[6] a) S. V. Eliseeva, J.-C. G. Bünzli, *Chem. Soc. Rev.* **2010**, *39*, 189–227; b) J.-C. G. Bünzli, S. V. Eliseeva, *J. Rare Earth* **2010**, *28*, 824–842; c) S. Pandya, J. Yu, D. Parker, *Dalton Trans.* **2006**, 2757; d) S. Faulkner, S. J. A. Pope, B. P. Burton-Pye, *Appl. Spectrosc. Rev.* **2005**, *40*, 1.
[7] For recent examples see: a) H. He, L. Si, Y. Zhong, M. Dubey, *Chem. Commun.* **2012**, *48*, 1886–1888, and references therein.
[8] For reviews see: a) C. Andraud, O. Maury, *Eur. J. Inorg. Chem.* **2009**, 4357–4371; b) Y. Ma, Y. Wang, *Coord. Chem. Rev.* **2010**, *254*, 972–990.
[9] G. Piszczek, I. Gryczynski, B. P. Maliwal, J. R. Lakowicz, *J. Fluoresc.* **2002**, *12*, 15–17.
[10] T. Zhang, X. Zhu, C. C. W. Cheng, W. M. Kwok, H. L. Tam, J. Hao, D. W. J. Kwong, W. K. Wong, K. L. Wong, *J. Am. Chem. Soc.* **2011**, *133*, 20120–20122.
[11] a) A. D'Aléo, A. Picot, A. Beeby, J. A. G. Williams, B. Le Guennic, C. Andraud, O. Maury, *Inorg. Chem.* **2008**, *47*, 10258–10268; b) A. D'Aléo, A. Picot, P. L. Baldeck, C. Andraud, O. Maury, *Inorg. Chem.* **2008**, *47*, 10269–10279.
[12] A. Picot, A. D'Aléo, P. L. Baldeck, A. Grichine, A. Duperray, C. Andraud, O. Maury, *J. Am. Chem. Soc.* **2008**, *130*, 1532–1533.
[13] G. Nocton, A. Nonat, C. Gateau, M. Mazzanti, *Helv. Chim. Acta* **2009**, *92*, 2257–2273.
[14] A. Bourdolle, M. Allali, J.-C. Mulatier, B. Le Guennic, J. Zwier, P. L. Baldeck, J.-C. G. Bünzli, C. Andraud, L. Lamarque, O. Maury, *Inorg. Chem.* **2011**, *50*, 4987–4999.
[15] For mono-metallic complexes see: a) E. G. Moore, J. Xu, S. C. Dodoni, C. J. Jocher, A. D'Aléo, M. Seitz, K. Raymond, *Inorg. Chem.* **2010**, *49*, 4156–4166; b) A. Nonat, D. Imbert, J. Pecaut, M. Giraud, M. Mazzanti, *Inorg. Chem.* **2009**, *48*, 4207–4218; c) S. Comby, D. Imbert, C. Vandevyver, J.-C. G. Bünzli, *Chem. Eur. J.* **2007**, *13*, 936–944; d) M. H. V. Werts, R. H. Woudenberg, P. G. Emmerink, R. van Gassel, J. W. Hofstraat, J. W. Verhoeven, *Angew. Chem.* **2000**, *112*, 4716–4718; *Angew. Chem. Int. Ed.* **2000**, *39*, 4542–4544.
[16] a) P. M. Allen, W. Liu, V. P. Chauhan, J. Lee, A. Y. Ting, D. Fukumura, R. K. Jain, M. G. Bawendi, *J. Am. Chem. Soc.* **2010**, *132*, 470–471; b) D. Kobat, M. E. Durst, N. Nishimura, A. W. Wong, C. B. Schaffer, C. Xu, *Opt. Express* **2009**, *17*, 13354–13364.
[17] No images could be obtained using **Yb[1]** as probe certainly because of its too low stability in the small animal.